J. Fluid Mech. (1983), *vol.* 134, *pp.* 67–83
Printed in Great Britain

The destruction of temperature fluctuations in a turbulent plane jet

By R. A. ANTONIA AND L. W. B. BROWNE
Department of Mechanical Engineering, University of Newcastle, N.S.W., 2308, Australia

(Received 2 June 1982 and in revised form 10 March 1983)

The transport equation for the destruction of temperature fluctuations in a turbulent shear flow is briefly discussed from the point of view of the experimenter's ability to measure the important terms. The transport equation for only one component of the destruction, the mean-square streamwise temperature derivative, is considered in detail in the case of a steady two-dimensional turbulent shear flow. Measurements of most of the terms in this equation have been made in the self-preserving region of a turbulent plane jet. They indicate that the advection and diffusion terms are negligible compared with the production and dissipation terms. The measured terms are discussed in the context of local isotropy. Mean-square values of second-order derivatives satisfy local isotropy more closely than those of first-order derivatives.

1. Introduction

A characteristic timescale τ_u of velocity fluctuations in a turbulent flow is given by the ratio $\overline{q^2}/\bar{\epsilon}$, where $\overline{q^2}$ ($\equiv \overline{u^2}+\overline{v^2}+\overline{w^2}$) is twice the turbulent kinetic energy and $\bar{\epsilon}$ is the average rate of dissipation of $\frac{1}{2}\overline{q^2}$. Analogously, a characteristic timescale τ_θ of temperature fluctuations may be written as $\overline{\theta^2}/\overline{N}$, where $\overline{\theta^2}$ is the mean-square temperature fluctuation and $\overline{N}$ (sometimes the symbols $\bar{\chi}$ or $\bar{\epsilon}_\theta$ are used) is the rate of dissipation of $\frac{1}{2}\overline{\theta^2}$; i.e. $\overline{N} = \alpha\overline{(\partial\theta/\partial x_j)^2}$, where α is the thermal diffusivity and the summation convention on repeated indices is understood. The ratio τ_θ/τ_u was found (Béguier, Dekeyser & Launder 1978) to be nearly uniform with a value close to 0.5 in several thin shear flows provided that the velocity and thermal fields have common origins. These flows include wall turbulence, where the budgets of $\frac{1}{2}\overline{q^2}$ and $\frac{1}{2}\overline{\theta^2}$ are dominated by production and dissipation, and free shear flows, where production and dissipation remain the principal terms of the budgets. Béguier *et al.* (1978) and Newman, Launder & Lumley (1981) also pointed out that τ_θ/τ_u will not, in general, be constant. Launder (1976) reported a twofold variation in τ_θ/τ_u for only a narrow span of flows and concluded that the ratio τ_θ/τ_u is not sufficiently constant to serve as a general method for determining $\overline{N}$.

Transport equations for $\overline{N}$ and $\overline{\theta^2}$ should in principle lead to a useful second-order closure model for heat and concentration transfer. Newman *et al.* (1981) proposed an approximate transport equation for $\overline{N}$ and reported satisfactory agreement of the model with a limited number of homogeneous scalar flows. Elghobashi & Launder (1981) showed that this model also correctly simulated the spread of a thermal mixing layer behind a half-heated grid. The experimenter's ability to measure all three components of $\overline{N}$ (e.g. Freymuth & Uberoi 1971; Sreenivasan, Antonia & Danh 1977) is extremely important from the point of view of providing experimental verification of the transport equation for $\overline{N}$. Without this ability, the verification would be constrained by the use of local isotropy.

The equation for $\overline{N}$ is briefly discussed in §2, not with an intention of modelling, but primarily with a view to assess the experimenter's ability to measure its terms. The transport equation for one component of $\overline{N}$, the mean-square streamwise derivative of temperature $\overline{(\partial\theta/\partial x)^2}$, is considered in more detail and it is ascertained that most of the terms are accessible to measurement using standard hot-wire and cold-wire techniques. These terms have been measured in the self-preserving region of a turbulent plane jet. The experimental techniques used and the difficulties associated with the derivative measurements are discussed in §3. The measurements are presented and discussed in §4. Implications with regard to local isotropy are also discussed.

2. Transport equations for $\overline{N}$ and $\overline{(\partial\theta/\partial x)^2}$

The transport equation for $\alpha\overline{(\partial\theta/\partial x_j)^2}$ or $\overline{N}$ can be derived (e.g. Corrsin 1953) from the equation for instantaneous temperature fluctuation (obtained by subtracting the equation for the incompressible mean heat-transfer rate from the Reynolds form of the instantaneous heat-transfer equation)

$$\frac{\partial\theta}{\partial t}+u_i\frac{\partial\overline{T}}{\partial x_i}+\overline{U}_i\frac{\partial\theta}{\partial x_i}+u_i\frac{\partial\theta}{\partial x_i}-\overline{u_i\frac{\partial\theta}{\partial x_i}}=\alpha\frac{\partial^2\theta}{\partial x_i\,\partial x_i}, \tag{1}$$

where $\overline{U}_i$ is the mean velocity and $\overline{T}$ is the mean temperature. Differentiating (1) with respect to x_j, multiplying the resulting equation by $\alpha\,\partial\theta/\partial x_j$ and averaging yields the transport equation for $\overline{N}$. For a steady flow,

$$\underset{\text{I}}{\overline{U}_i\frac{\partial\overline{N}}{\partial x_i}}+\underset{\text{II}}{2\alpha\overline{u_i\frac{\partial\theta}{\partial x_j}\frac{\partial^2\overline{T}}{\partial x_i\,\partial x_j}}}+\underset{\text{III}}{2\alpha\overline{\frac{\partial\theta}{\partial x_i}\frac{\partial\theta}{\partial x_j}\frac{\partial\overline{U}_i}{\partial x_j}}}+\underset{\text{IV}}{\frac{\partial}{\partial x_i}\overline{(u_i N)}}$$

$$+\underset{\text{V}}{2\alpha\overline{\frac{\partial\theta}{\partial x_i}\frac{\partial\theta}{\partial x_j}\frac{\partial u_i}{\partial x_j}}}+\underset{\text{VI}}{2\alpha\overline{\frac{\partial\theta}{\partial x_j}\frac{\partial u_i}{\partial x_j}}\frac{\partial\overline{T}}{\partial x_i}}-\underset{\text{VII}}{2\alpha^2\overline{\frac{\partial\theta}{\partial x_j}\nabla^2\left(\frac{\partial\theta}{\partial x_j}\right)}}=0, \tag{2}$$

where ∇^2 is the Laplacian $\partial^2/\partial x_i\,\partial x_i$. The temperature-gradient-fluctuation equation (2) was derived by Corrsin (1953), who compared it with the vorticity-fluctuation equation. Corrsin noted the existence of apparently significant differences between these two equations, but pointed out that a closer analogy existed between the behaviour of $(\partial\theta/\partial x_j)^2$, rather than θ itself, and that of vorticity. Corrsin suggested a tentative physical interpretation of terms I–IV and term VII in (2) by analogy to corresponding terms in the transport equation for $\overline{\theta^2}$. Equation (2) was also discussed by Lumley & Khajeh-Nouri (1974) (see also Launder 1976). Wyngaard (1971) considered the locally isotropic form of (2) for high-Reynolds-number stationary turbulence. In this form, (2) essentially reduces to a balance between V and VII (see also Tennekes & Lumley 1972). Term V represents the production of $\overline{(\partial\theta/\partial x_i)^2}$ due to the stretching of the temperature field by the turbulent strain field. Term VII is identified with the molecular smoothing of the temperature gradient field.

An order-of-magnitude argument† (e.g. Tennekes & Lumley 1972; Owen 1973) can

† While conventional order-of-magnitude arguments provide a useful indication of the magnitude of the terms of (2), they become somewhat tenuous when all the terms in the transport equation reduce to zero when local isotropy is involved. This occurs when the transport equation for $(\partial\theta/\partial x)^3$ is considered (Wyngaard 1976; Sreenivasan & Tavoularis 1980).

be used to show that terms V and VII, which involve interactions between fine-scale temperature and/or velocity fluctuations, are the dominant terms of (2), at least for sufficiently large Reynolds and Péclet numbers. These terms can be interpreted as the production and dissipation terms respectively for $\overline{N}$. Term V is of order $\alpha u_s \theta_s^2/\lambda^3$, where u_s and θ_s are characteristic velocity and temperature scales respectively, and λ is the Taylor microscale. Strictly V is $O(\alpha u_s \theta_s^2/\lambda_\theta^2 \lambda)$, where λ_θ is the temperature microscale analogous to λ. For present purposes, the molecular Prandtl number is assumed equal to unity and no distinction is made between λ_θ and λ. Terms I and IV are $O(\alpha u_s \theta_s^2/l\lambda^2)$, where l is an integral lengthscale of the turbulence, and hence of order R_λ ($\equiv u_s\lambda/\nu$) smaller than V. Terms III and VI are $O(\alpha u_s \theta_s^2/\lambda^2 l)$ and hence of the same order as I or IV. Term II is $O(\alpha u_s \theta_s^2/\lambda l^2)$, hence $O(R_\lambda)$ smaller than I or IV and will not be considered further. To $O(R_\lambda)$ or $O(u_s l/\nu)^{\frac{1}{2}}$ all terms except II need to be considered. From a modelling point of view, since the difference between V and VII is $O(u_s l/\nu)^{-\frac{1}{2}}$, a useful predictive equation should also contain the terms I, III, IV and VI, which are of this order.

The instantaneous value of N can be obtained with two pairs of parallel wires, an arrangement investigated by Sreenivasan *et al.* (1977). This arrangement is somewhat cumbersome and would lead to spatial resolution constraints if used in conjunction with an X-probe, as required for the measurement of several terms of (2).

Denoting components of u_i in the usual (x, y, z) coordinate system by u, v and w, the simultaneous measurement of $\partial\theta/\partial y$ and $\partial\theta/\partial z$ is required for the correlations $\overline{(\partial\theta/\partial y)\,(\partial\theta/\partial z)\,(\partial v/\partial z)}$ and $\overline{(\partial\theta/\partial y)\,(\partial\theta/\partial z)\,(\partial w/\partial y)}$ which form part of the production term (see (3)). It would seem that only one pair of parallel cold wires, which may be rotated to yield $\partial\theta/\partial y$ and $\partial\theta/\partial z$ separately, is sufficient for the measurement of many terms in (2). We should, however, focus our attention on the important terms V and VII of (2). Term V can be expanded as

$$2\alpha\overline{\frac{\partial\theta}{\partial x_i}\frac{\partial\theta}{\partial x_j}\frac{\partial u_i}{\partial x_j}} = 2\alpha\left\{\overline{\frac{\partial u}{\partial x}\left(\frac{\partial\theta}{\partial x}\right)^2} + \overline{\frac{\partial\theta}{\partial x}\frac{\partial\theta}{\partial y}\frac{\partial v}{\partial x}} + \overline{\frac{\partial\theta}{\partial x}\frac{\partial\theta}{\partial z}\frac{\partial w}{\partial x}}\right.$$
$$+ \overline{\frac{\partial\theta}{\partial x}\frac{\partial\theta}{\partial y}\frac{\partial u}{\partial y}} + \overline{\frac{\partial\theta}{\partial x}\frac{\partial\theta}{\partial z}\frac{\partial u}{\partial z}} + \overline{\left(\frac{\partial\theta}{\partial y}\right)^2\frac{\partial v}{\partial y}}$$
$$\left. + \overline{\left(\frac{\partial\theta}{\partial z}\right)^2\frac{\partial w}{\partial z}} + \overline{\frac{\partial\theta}{\partial y}\frac{\partial\theta}{\partial z}\frac{\partial v}{\partial z}} + \overline{\frac{\partial\theta}{\partial y}\frac{\partial\theta}{\partial z}\frac{\partial w}{\partial y}}\right\}. \quad (3)$$

With the assumption that terms involving $\partial/\partial x$ can be inferred from time derivatives using Taylor's hypothesis ($\partial/\partial x \equiv -U^{-1}\partial/\partial t$), the first three terms on the right can be obtained by placing one X-probe next to one pair of cold wires. The following two terms require one pair of hot wires next to one pair of cold wires. The sixth and seventh terms involve derivatives in the y- and z-directions and require two X-probes (their replacement with two V-probes may lead to an improvement in spatial resolution) next to one pair of cold wires. The measurement of the last two terms is more complicated as two X-probes (or V-probes) and two pairs of parallel wires would be required.

Term VII can be rewritten as

$$-2\alpha^2\overline{\frac{\partial\theta}{\partial x_j}\nabla^2\left(\frac{\partial\theta}{\partial x_j}\right)} = 2\alpha^2\overline{\left(\frac{\partial^2\theta}{\partial x_i\,\partial x_j}\right)^2} - \alpha^2\nabla^2\overline{\left(\frac{\partial\theta}{\partial x_j}\right)^2}, \quad (4)$$

where the second term on the right could be physically interpreted as the molecular diffusion of temperature-gradient-fluctuation intensity by conduction. This term is, however, negligible compared with the first, using the order-of-magnitude argument

which was previously applied to (2). Components of $\overline{(\partial^2\theta/\partial x_i\,\partial x_j)^2}$ that include $\partial/\partial x$ are obtainable using Taylor's hypothesis, but components that include derivatives in the y- and/or z-directions are less easily obtainable.

Significant reduction in the complexity of measurement results by considering only the streamwise component of (2). The transport equation for $\overline{(\partial\theta/\partial x)^2}$ can be obtained from (2) by putting $j = 1$ and dividing by α. When the mean flow is two-dimensional, this equation is (the numbering in (2) is retained)

$$\underbrace{\overline{U}\frac{\partial}{\partial x}\overline{\left(\frac{\partial\theta}{\partial y}\right)^2}+\overline{V}\frac{\partial}{\partial y}\overline{\left(\frac{\partial\theta}{\partial x}\right)^2}}_{\text{I}}+\underbrace{2\overline{\left(\frac{\partial\theta}{\partial x}\right)^2}\frac{\partial\overline{U}}{\partial x}+2\frac{\overline{\partial\theta}\,\overline{\partial\theta}\,\partial\overline{V}}{\partial x\,\partial y\,\partial x}}_{\text{III}}$$

$$+\underbrace{\frac{\partial}{\partial x}\overline{u\left(\frac{\partial\theta}{\partial x}\right)^2}+\frac{\partial}{\partial y}\overline{v\left(\frac{\partial\theta}{\partial x}\right)^2}}_{\text{IV}}+\underbrace{2\overline{\left(\frac{\partial\theta}{\partial x}\right)^2}\frac{\partial u}{\partial x}+2\frac{\overline{\partial v\,\partial\theta\,\partial\theta}}{\partial x\,\partial x\,\partial y}+2\frac{\overline{\partial w\,\partial\theta\,\partial\theta}}{\partial x\,\partial x\,\partial z}}_{\text{V}}$$

$$+\underbrace{2\frac{\overline{\partial u\,\partial\theta}\,\partial\overline{T}}{\partial x\,\partial x\,\partial x}+2\frac{\overline{\partial v\,\partial\theta}\,\partial\overline{T}}{\partial x\,\partial x\,\partial y}}_{\text{VI}}+\underbrace{2\alpha\left\{\overline{\left(\frac{\partial^2\theta}{\partial x^2}\right)^2}+\overline{\left(\frac{\partial^2\theta}{\partial x\,\partial y}\right)^2}+\overline{\left(\frac{\partial^2\theta}{\partial x\,\partial z}\right)^2}\right\}}_{\text{VII}}=0. \tag{5}$$

Only x-derivatives of velocity components appear in the correlations in (5), so that only one X-probe is required, assuming Taylor's hypothesis. While all terms in (5) are, in principle, accessible to hot- and cold-wire techniques, the second and third components of V have not been measured in the present investigation as their measurement would require unavoidably large separations between velocity and temperature sensors. Their value is estimated by assuming local isotropy (see (6)).

3. Experimental arrangement and conditions

A detailed description of the jet facility and instrumentation is given in Antonia *et al.* (1983). It is sufficient to note here that the jet issues from a nozzle of width $d = 12.7$ mm and height 25 cm. Two confining horizontal plates are located at the top and bottom of the nozzle to help maintain the two-dimensionality of the flow. The present measurements were made at a distance x from the nozzle equal to $40d$. The jet Reynolds number based on d is 7620. The jet was heated to a temperature at the nozzle exit of about 25 °C above ambient. The flow was approximately self-preserving for $x/d \gtrsim 20$.

Fluctuations u, v were measured with an X-probe with 2.5 μm Pt wires of about 0.4 mm in length and separated by about 0.4 mm. The same X-probe was rotated through 90° to allow measurements of w. The wires were operated with constant-temperature anemometers at an overheat of 0.8. A 0.63 μm (Pt–10 % Rh) cold wire was located 0.4 mm upstream of the centre of the X-probe and perpendicular to the plane of the X-probe. Transverse derivatives of temperature were estimated by subtracting the signals of two parallel cold wires (0.63 μm diameter, 0.43 mm long, separated by 0.47 mm, the resistances of these wires were matched to better than 0.5 %). The cold wires were operated as resistance thermometers with constant-current (0.1 mA) circuits.

Mestayer & Chambaud (1979) noted that errors associated with the use of parallel

cold wires could arise from a possible difference between wire time constants and possible errors in estimating the temperature sensitivities of the wires. The latter possibility was minimized by carrying out the temperature calibration of the wire pair (and associated electronics) in the jet exit plane. The frequency response of the cold wires was estimated using the pulsed-wire technique of Antonia, Browne & Chambers (1981) to extend beyond the Kolmogorov frequency f_K ($= U/2\pi l_K$, where l_K is the Kolmogorov microscale). Since the cold-wire signals were filtered (see below) at a frequency slightly smaller than f_K, the error was considered to be negligible.

For the X-probe/cold-wire arrangement, the analog voltages from the constant-temperature and constant-current anemometers were first recorded on analog tape and subsequently digitized. The temperature contamination of the hot-wire signals was removed and these signals were subsequently linearized by the computer. Differentiation of these signals and of the cold-wire signal were also implemented using the computer. For the parallel cold-wire arrangement, analog circuits were used to obtain $\partial/\partial t$ and the difference, proportional to $\partial\theta/\partial y$ or $\partial\theta/\partial z$, between the cold-wire voltages. These voltages were low-pass filtered with a cutoff frequency f_c equal to about $0.9f_K$ and subsequently digitized at a frequency equal to $2f_c$. The magnitude of f_c depends on the signal-to-noise ratio of the wire (equal to about 7 in the case of $\partial\theta/\partial t$ and about 5 for $\partial\theta/\partial y$ or $\partial\theta/\partial z$ for the 0.63 μm wires).† The selection of f_c followed inspection of the spectrum of $\partial\theta/\partial t$; the frequency at which this spectrum merged with the noise spectrum (obtained and stored in a real-time spectrum analyser when the wire was in the jet exit plane) was first identified and f_c was subsequently set at a frequency (smaller than that at which merging occurred) corresponding to about 2 dB above that of the merging frequency. Since it is desirable that f_c is at least equal to f_K, some attenuation of the high-frequency end of the spectra of derivatives would be expected. To compensate for this effect, $\partial\theta/\partial t$ was also obtained with a 0.25 μm Pt–10% Rh cold wire (length $\approx$ 0.22 mm, current = 0.05 mA). In view of the improved signal-to-noise ratio, the differentiated output from this wire was filtered at $f_c = 1.2f_K$. The length of this wire was sufficiently comparable to the Kolmogorov scale to ignore wire-length corrections. Values of $\overline{(\partial u/\partial t)^2}$ and f_K were determined using a single hot wire (1.3 μm Pt, length = 0.22 mm) for which wire-length corrections were also negligible. While the magnitudes of the ratios $\overline{(\partial\theta/\partial y)^2}/\overline{(\partial\theta/\partial x)^2}$ and $\overline{(\partial\theta/\partial z)^2}/\overline{(\partial\theta/\partial x)^2}$ were determined from the parallel 0.63 μm wires, absolute values of $\overline{(\partial\theta/\partial y)^2}$ and $\overline{(\partial\theta/\partial z)^2}$ were calculated using the value of $\overline{(\partial\theta/\partial x)^2}$ obtained with the 0.25 μm cold wire. Similarly, absolute values of correlations that include the velocity derivative $\partial u/\partial x$ were inferred using the value of $\overline{(\partial u/\partial x)^2}$ obtained with the 1.3 μm hot wire. For consistency, the relative magnitudes of the three components of the dissipation term in (5) were determined from spectra of $\partial\theta/\partial t$, $\partial\theta/\partial y$, $\partial\theta/\partial z$ obtained with the parallel 0.63 μm cold wires. The absolute magnitudes of these components were calculated using the values of $\overline{(\partial\theta/\partial x)^2}$ obtained with the 0.25 μm cold wire.

Streamwise derivatives of velocity and temperature have been inferred from temporal derivatives using Taylor's hypothesis. Available corrections (e.g. Wyngaard & Clifford 1977) for the effect of a fluctuating convection velocity on Taylor's hypothesis and hence on the mean squared values of $\partial\theta/\partial x$ and $\partial^2\theta/\partial x^2$ were not applied for reasons discussed in Antonia *et al.* (1981) and Browne, Antonia & Rajagopalan (1982).

On the jet centreline at $x/d = 40$, R_λ (obtained by substituting $(\overline{u^2})^{\frac{1}{2}}$ for u_s) is about

† Mean-square values of the derivatives and differences were corrected by subtracting, on a mean-square basis, contributions from the noise.

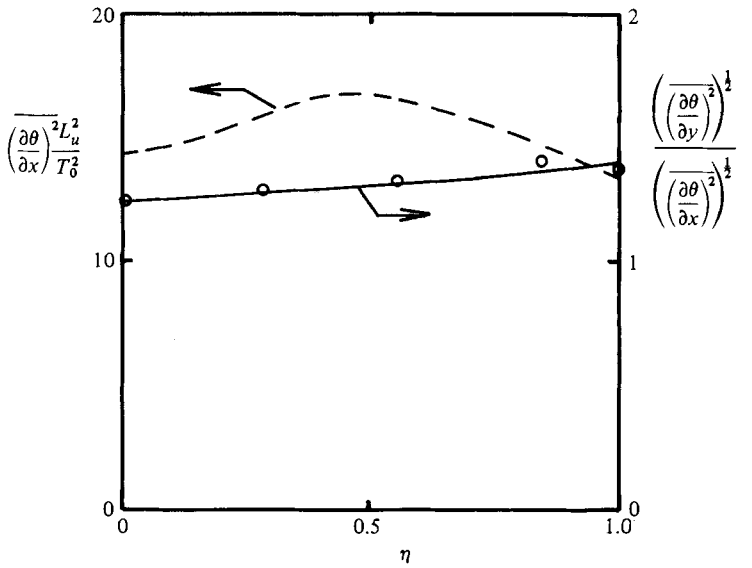

FIGURE 1. Mean-square temperature derivatives and ratio of r.m.s. derivatives in x- and y-directions: ---, $\overline{(\partial\theta/\partial x)^2} L_u^2/T_0^2$; ——, $\{\overline{(\partial\theta/\partial y)^2}/\overline{(\partial\theta/\partial x)^2}\}^{\frac{1}{2}}$.

190, the Péclet number ($\equiv \overline{(u^2)}^{\frac{1}{2}} \lambda_\theta/\alpha$, where $\lambda_\theta = \overline{(\theta^2)}^{\frac{1}{2}}/\overline{(\partial\theta/\partial x)^2}^{\frac{1}{2}}$) is about 100, the Kolmogorov scale l_K is 0.16 mm. The mean temperature T_0, relative to ambient, is 9 °C, while the mean velocity U_0 is 3.4 m/s. The jet velocity half-width L_u is 60 mm. The ratios $\overline{(u^2)}^{\frac{1}{2}}/U_0$, $\overline{(v^2)}^{\frac{1}{2}}/U_0$ and $\overline{(w^2)}^{\frac{1}{2}}/U_0$ are equal to about 0.18, 0.14 and 0.15 respectively at the centreline.

Flow reversal was first detected at a distance y from the jet centreline equal to about L_u. When reversal occurs, the thermal wakes from the X-probe wires contaminate the signal from the cold wire upstream of the X-probe. Both the intensity and frequency of contamination increase as η ($\equiv y/L_u$) increases, with a consequent impairment of the accuracy of measurement. For this reason, data extending only to $\eta \approx 1$ are presented in §4.

4. Results and discussion

Before discussing the equation for $\overline{(\partial\theta/\partial x)^2}$, it seems appropriate to note that $\overline{N}$ was obtained (Antonia *et al.* 1983) by measuring all three components. The distribution, over the jet half-width, of $\overline{(\partial\theta/\partial x)^2}$, normalized by L_u and T_0, is shown in figure 1. The components $\overline{(\partial\theta/\partial y)^2}$ and $\overline{(\partial\theta/\partial z)^2}$ are roughly equal but larger than $\overline{(\partial\theta/\partial x)^2}$. The ratio $\{\overline{(\partial\theta/\partial y)^2}/\overline{(\partial\theta/\partial x)^2}\}^{\frac{1}{2}}$ (figure 1) increased from about 1.24 at $\eta = 0$ to 1.4 at $\eta = 1$. On the basis of these measurements local isotropy is violated. The magnitude of $\overline{N}$ did, however, lead to a satisfactory closure (figure 2) of the budget for $\frac{1}{2}\overline{\theta^2}$, providing support for the observed inequality between $\overline{(\partial\theta/\partial x)^2}$ and $\overline{(\partial\theta/\partial y)^2}$ or $\overline{(\partial\theta/\partial z)^2}$. This inequality has been observed in a boundary layer (Sreenivasan *et al.* 1977; Verollet 1972) and in a quasihomogeneous turbulent shear flow (Tavoularis & Corrsin 1981). By contrast, Freymuth & Uberoi's (1971) budget of $\overline{\theta^2}$ in the two-dimensional wake of a cylinder indicated approximate equality between the three components of $\overline{N}$ and good closure for the budget.

The terms of (5), normalized by multiplying with $L_u^3/U_0 T_0^2$, have been obtained by assuming self-preserving distributions for the time-averaged quantities and using

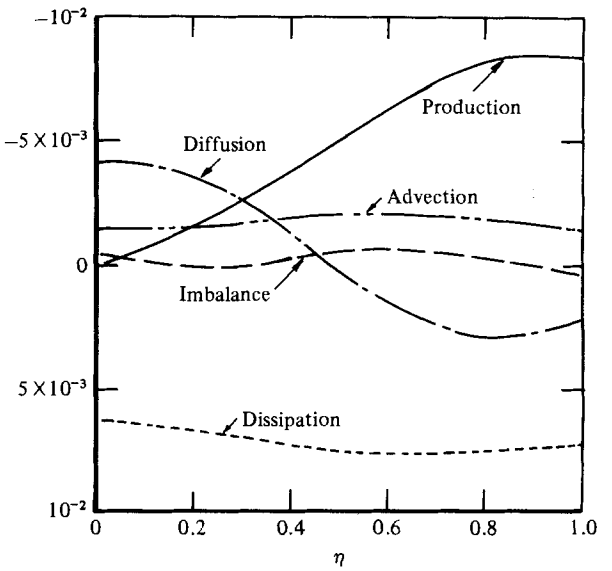

FIGURE 2. Measured budget of $\frac{1}{2}\overline{\theta^2}$. All terms of the budget have been multiplied by $L_u/U_0T_0^2$.

the experimentally determined values of $\mathrm{d}L_u/\mathrm{d}x$, $\mathrm{d}T_0/\mathrm{d}x$ and $\mathrm{d}U_0/\mathrm{d}x$ to estimate derivatives with respect to x and y for derivatives of these time-averaged quantities. For example, the advection term I can be written

$$\frac{L_u^3}{U_0T_0^2}\left\{\overline{U}\frac{\partial}{\partial x}\overline{\left(\frac{\partial\theta}{\partial x}\right)^2}+\overline{V}\frac{\partial}{\partial y}\overline{\left(\frac{\partial\theta}{\partial y}\right)^2}\right\}=-\frac{\mathrm{d}L_u}{\mathrm{d}x}(\eta gf'+2fg)+2fg\left(\frac{L_u}{T_0}\frac{\mathrm{d}T_0}{\mathrm{d}x}\right)+kf',$$

where

$$\overline{U}=U_0g(\eta),\quad \overline{V}=U_0k(\eta),\quad \overline{\left(\frac{\partial\theta}{\partial x}\right)^2}=\frac{T_0^2}{L_u^2}f(\eta),$$

and experimental values of $\mathrm{d}L_u/\mathrm{d}x$ ($=0.104$) and $(L_u/T_0)\,\mathrm{d}T_0/\mathrm{d}x$ ($=-0.04$) were used. The functions g, k and f were obtained using cubic-spline least-square fits to the data for $\overline{U}/U_0$, $\overline{V}/U_0$† and $\overline{(\partial\theta/\partial x)^2}\,L_u^2/T_0^2$ at $x/d=40$. The distribution for f' was determined by numerically differentiating the fit for f and subsequently applying a least-square fit to estimates for the derivative. Expressions for other terms in (5) were obtained by following an analogous procedure. Individual data points are not shown in all the figures. It should be noted, however, that the curves shown in these figures were either fitted to or derived from best fits to a minimum of 5 and a maximum of 8 data points in the range $0\leqslant\eta\leqslant1$. Some idea of the experimental scatter can be seen from figure 3, where the data points are shown together with the least-square fits for the correlations which appear in term IV.

Distributions for terms I, III, IV and VI are shown in figure 4. All terms contribute to a production of $\overline{(\partial\theta/\partial x)^2}$ (the production term V is negative) in the region $0\leqslant\eta\lesssim0.5$. Both III and IV become positive when $\eta\gtrsim0.5$. Of the four terms plotted, the advection (term I) or convection of $\overline{(\partial\theta/\partial x)^2}$ by the mean velocity is clearly the largest. The magnitude of term VI, which represents the interaction between the mean-temperature gradient and the fine-scale velocity and temperature fields, is small everywhere in the range $0\leqslant\eta\leqslant1$. The distribution of term III, which represents

† $\overline{V}$ was obtained using continuity.

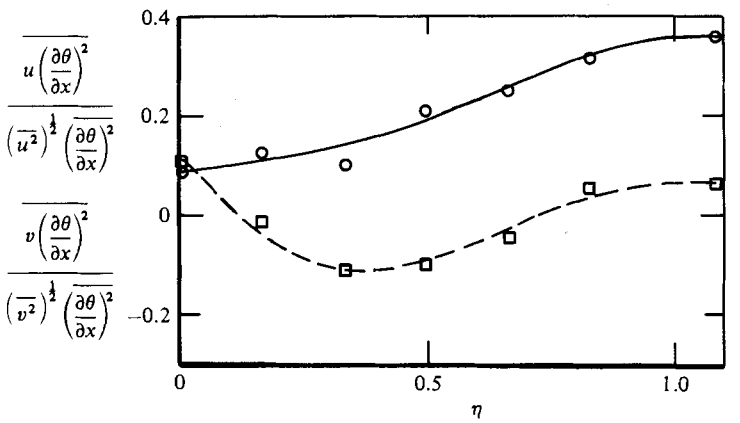

FIGURE 3. Correlation between velocity fluctuations and $\overline{(\partial\theta/\partial x)^2}$: ○, $\overline{u(\partial\theta/\partial x)^2}/\overline{(u^2)^{\frac{1}{2}}}\,\overline{(\partial\theta/\partial x)^2}$; □, $\overline{v(\partial\theta/\partial x)^2}/\overline{(v^2)^{\frac{1}{2}}}\,\overline{(\partial\theta/\partial x)^2}$. Symbols are individual data points; curves are least-square fits.

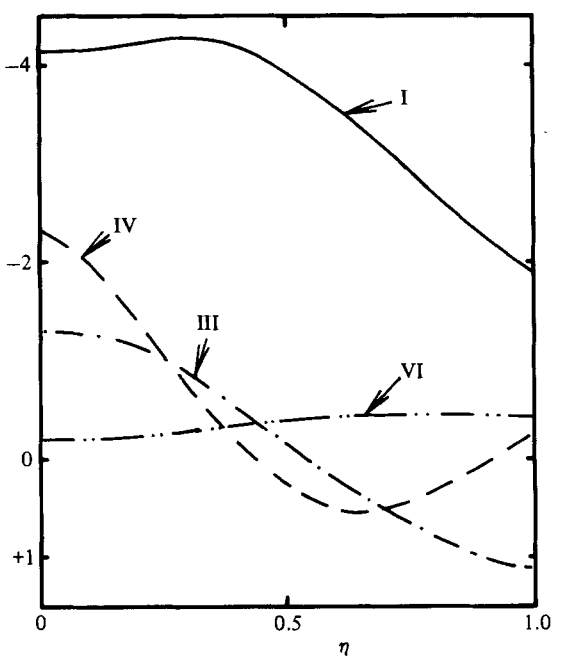

FIGURE 4. Terms I, III, IV and VI in (5), normalized by $L_u^3/U_0 T_0^2$.

an interaction between the longitudinal mean strain rate† and the fine-scale temperature field, is somewhat similar to that of term IV. This latter term could be interpreted as the diffusion or transport of $\overline{(\partial\theta/\partial x)^2}$ by the turbulent velocity field. Its magnitude has a maximum value at $\eta = 0$, but, in contrast to the budget of $\overline{\theta^2}$ where diffusion is almost three times as large as the advection, this maximum is about half the magnitude of the advection.

The correlations in term VI and the second correlation in III should be zero if local isotropy is invoked. The experimental distributions for these correlations are shown

† Note that $\partial\overline{U}/\partial y$ does not appear in (5).

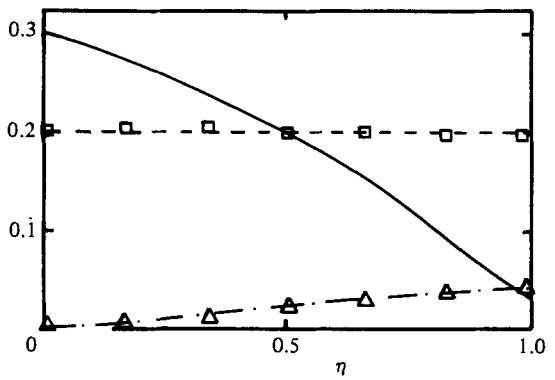

FIGURE 5. Correlation coefficients between velocity and/or temperature derivatives: ——, $-\overline{(\partial\theta/\partial x)(\partial\theta/\partial y)}/((\overline{\partial\theta/\partial x})^2)^{\frac{1}{2}}(\overline{(\partial\theta/\partial y)^2})^{\frac{1}{2}}$; – – –, $\overline{(\partial u/\partial x)(\partial\theta/\partial x)}/((\overline{\partial u/\partial x})^2)^{\frac{1}{2}}(\overline{(\partial\theta/\partial x)^2})^{\frac{1}{2}}$; —·—, $\overline{(\partial v/\partial x)(\partial\theta/\partial x)}/((\overline{\partial v/\partial x})^2)^{\frac{1}{2}}(\overline{(\partial\theta/\partial x)^2})^{\frac{1}{2}}$. Symbols are individual data points; curves are least-square best fits.

in figure 5. The correlation coefficient between $\partial v/\partial x$ and $\partial\theta/\partial x$ is negligible near the jet centreline. The correlation coefficient between $\partial u/\partial x$ and $\partial\theta/\partial x$ remains constant, equal to about 0.2, across the jet. The correlation coefficient between $\partial\theta/\partial x$ and $\partial\theta/\partial y$ is large, especially at the centreline. For comparison, Tavoularis & Corrsin (1981) obtained a value for this coefficient of -0.48 in a quasihomogeneous shear flow with a constant mean-temperature gradient. The Reynolds and Péclet numbers in Tavoularis & Corrsin's investigations are comparable to those in the present experiment.

The present measurements for the correlation coefficient between $\partial u/\partial x$ and $(\partial\theta/\partial x)^2$ (component 1 of term V) indicate a magnitude of about 0.3 at $\eta = 0$. This value is in agreement with the previously reported (Van Atta 1974; Antonia & Chambers 1980) dependence of this coefficient on Reynolds number. The two other components of V were not measured but assumed to be those appropriate to local isotropy. The general isotropic form of the tensor $\overline{(\partial u_i/\partial x_j)(\partial\theta/\partial x_k)(\partial\theta/\partial x_m)}$ may be written as

$$\overline{\frac{\partial u_i}{\partial x_j}\frac{\partial\theta}{\partial x_k}\frac{\partial\theta}{\partial x_m}} = a\delta_{ij}\delta_{km} + b(\delta_{ik}\delta_{jm} + \delta_{im}\delta_{jk}) + c(\delta_{ik}\delta_{jm} - \delta_{im}\delta_{jk}).$$

Invariance with respect to reflection about the axes requires that $c = 0$. When $i = j$ and $k = m$, continuity ($\partial u_i/\partial x_i \equiv 0$) requires that $a = -\frac{2}{3}b$, so that

$$\overline{\frac{\partial u_i}{\partial x_j}\frac{\partial\theta}{\partial x_k}\frac{\partial\theta}{\partial x_m}} = b(\delta_{ik}\delta_{jm} + \delta_{im}\delta_{jk} - \tfrac{2}{3}\delta_{ij}\delta_{km}).$$

It follows that

$$\overline{\frac{\partial v}{\partial x}\frac{\partial\theta}{\partial x}\frac{\partial\theta}{\partial y}} = \overline{\frac{\partial w}{\partial x}\frac{\partial\theta}{\partial x}\frac{\partial\theta}{\partial z}} = \frac{3}{4}\overline{\left(\frac{\partial u}{\partial x}\right)\left(\frac{\partial\theta}{\partial x}\right)^2}. \tag{6}$$

Using these local isotropy relations, term V was calculated, and its distribution across the jet is shown in figure 10. A discussion is deferred until term VII has been considered.

Although all components of VII were measured, it is of interest to establish the relations between those components which satisfy local isotropy. Using a procedure

similar to that for the production term, the general isotropic form of the tensor $\overline{(\partial^2\theta/\partial x_i\,\partial x_j)\,(\partial^2\theta/\partial x_k\,\partial x_m)}$ is given by

$$\overline{\frac{\partial^2\theta}{\partial x_i\,\partial x_j}\frac{\partial^2\theta}{\partial x_k\,\partial x_m}} = a_1\,\delta_{ij}\,\delta_{km} + b_1\,\delta_{ik}\,\delta_{jm} + c_1\,\delta_{im}\,\delta_{jk}.$$

Since interchanging i and j or k and m does not alter the correlation, it follows that $b_1 = c_1$. If it is also noted that†

$$\overline{\frac{\partial}{\partial x_j}\left(\frac{\partial\theta}{\partial x_i}\frac{\partial^2\theta}{\partial x_k\,\partial x_m}\right)} = 0 = \overline{\frac{\partial^2\theta}{\partial x_i\,\partial x_j}\frac{\partial^2\theta}{\partial x_k\,\partial x_m}} + \overline{\frac{\partial\theta}{\partial x_i}\frac{\partial^3\theta}{\partial x_k\,\partial x_m\,\partial x_j}}, \tag{7}$$

$$\overline{\frac{\partial}{\partial x_k}\left(\frac{\partial\theta}{\partial x_i}\frac{\partial^2\theta}{\partial x_j\,\partial x_m}\right)} = 0 = \overline{\frac{\partial^2\theta}{\partial x_i\,\partial x_k}\frac{\partial^2\theta}{\partial x_j\,\partial x_m}} + \overline{\frac{\partial\theta}{\partial x_i}\frac{\partial^3\theta}{\partial x_k\,\partial x_m\,\partial x_j}}, \tag{8}$$

then subtracting (8) from (7) leads to

$$\overline{\left(\frac{\partial^2\theta}{\partial x_i\,\partial x_j}\right)\left(\frac{\partial^2\theta}{\partial x_k\,\partial x_m}\right)} = \overline{\left(\frac{\partial^2\theta}{\partial x_i\,\partial x_k}\right)\left(\frac{\partial^2\theta}{\partial x_j\,\partial x_m}\right)}.$$

The correlation thus remains unaltered when j and k are interchanged; thus $a_1 = b_1 = c_1$. It follows that

$$\overline{\left(\frac{\partial^2\theta}{\partial x^2}\right)^2} = 3\overline{\left(\frac{\partial^2\theta}{\partial x\,\partial y}\right)^2} = 3\overline{\left(\frac{\partial^2\theta}{\partial x\,\partial z}\right)^2}, \tag{9}$$

$$\overline{\left(\frac{\partial^2\theta}{\partial y\,\partial z}\right)^2} = \overline{\left(\frac{\partial^2\theta}{\partial x\,\partial z}\right)^2}.$$

Relation (9) can also be obtained by making use of the relationships, within the framework of local isotropy, between spectra of $\partial\theta/\partial x$ and $\partial\theta/\partial y$ or $\partial\theta/\partial z$. This approach is briefly given below since the second-order derivatives were estimated from the measured spectra of the first-order derivatives. The nth-order derivative of the temperature is related to ϕ_θ, the one-dimensional temperature spectrum, as follows

$$\overline{\left(\frac{\partial^n\theta}{\partial x^n}\right)^2} = \int_0^\infty k_1^{2n}\phi_\theta(k_1)\,\mathrm{d}k_1, \tag{10}$$

where k_1 is the one-dimensional wavenumber ($k_1 = \omega/\overline{U}$). It is more convenient to start with the spectrum ϕ_{θ_x} of $\partial\theta/\partial x$ ($\equiv \theta_x$; this notation is used only to identify spectra) rather than ϕ_θ, since the derivative $\partial\theta/\partial t$ was recorded during the experiment. It follows that

$$\overline{\left(\frac{\partial^2\theta}{\partial x^2}\right)^2} = \int_0^\infty \phi_{\theta_{xx}}(k_1)\,\mathrm{d}k_1 = \int_0^\infty k_1^2\,\phi_{\theta_x}(k_1)\,\mathrm{d}k_1, \tag{11}$$

where $\phi_{\theta_{xx}}$ is the spectrum of $\partial^2\theta/\partial x^2$ ($\equiv \theta_{xx}$). For isotropy,

$$\phi_{\theta_y}(k_1) = \phi_{\theta_z}(k_1). \tag{12}$$

It immediately follows that

$$\overline{\left(\frac{\partial^2\theta}{\partial x\,\partial y}\right)^2} = \overline{\left(\frac{\partial^2\theta}{\partial x\,\partial z}\right)^2}. \tag{13}$$

The relation between ϕ_{θ_y} or ϕ_{θ_z} and ϕ_{θ_x} has previously been established by Van Atta (1977):

$$\phi_{\theta_x}(k_1) = -k_1\frac{\partial\phi_{\theta_y}}{\partial k_1}. \tag{14}$$

† The authors are grateful to Dr Wyngaard for pointing out this step.

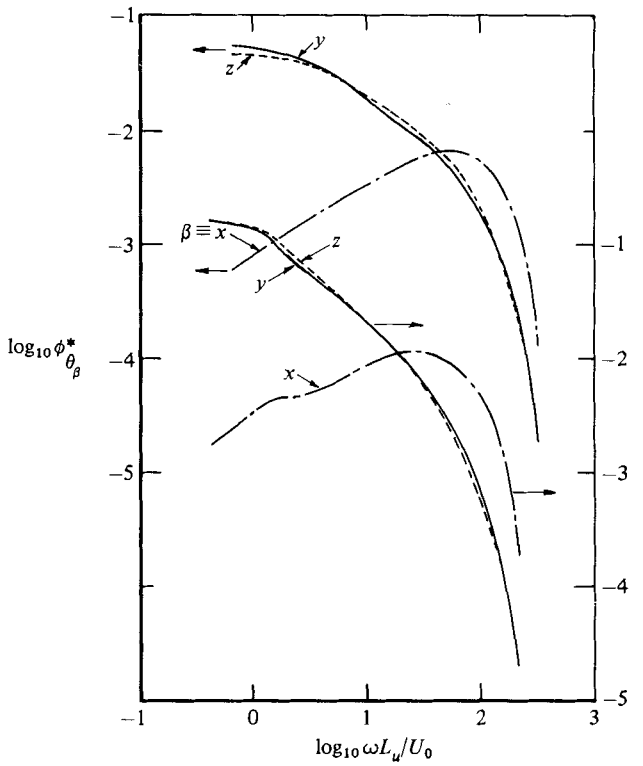

FIGURE 6. Spectral densities of the three temperature derivatives at $\eta = 0$ and 1. Upper and lower curves are for $\eta = 0$ and 1 respectively.

Using (11), (13) and (14), relation (9) follows, viz

$$\overline{\left(\frac{\partial^2\theta}{\partial x^2}\right)^2} = -[k_1^3\phi_{\theta_y}]_0^\infty + 3\int_0^\infty k_1^2\phi_{\theta_y}\,\mathrm{d}k_1 = 3\overline{\left(\frac{\partial^2\theta}{\partial x\,\partial y}\right)^2} = 3\overline{\left(\frac{\partial^2\theta}{\partial x\,\partial z}\right)^2}.$$

Experimental spectra of $\partial\theta/\partial x$, $\partial\theta/\partial y$ and $\partial\theta/\partial z$ at $\eta = 0$ and 1 are shown in figure 6 in terms of the normalised frequency $\omega L_u/U_0$. The asterisk on ϕ denotes normalization such that

$$\int_0^\infty \phi^*_{\theta_\beta}(k_1)\,\mathrm{d}k_1 = 1,$$

where $\beta \equiv x$, y or z. The relative behaviour of ϕ_{θ_x}, ϕ_{θ_y} and ϕ_{θ_z} is consistent with that previously reported by Sreenivasan *et al.* (1977) for the boundary layer. In particular, ϕ_{θ_y} and ϕ_{θ_z}, which are in good agreement with (12), are significantly richer in low-frequency content than ϕ_{θ_x}. Whereas ϕ_{θ_x} initially increases rapidly with k_1, ϕ_{θ_y} and ϕ_{θ_z} decrease monotonically with k_1. Distributions of $\phi^*_{\theta_x}$ multiplied by $(\omega L_u/U_0)^2$ are shown in figure 7 for $\eta = 0$ and 1, and are roughly symmetrical about the frequency at which the peak occurs. The distribution at $\eta = 0$ is equivalent to $\phi_{\theta_{xx}}$, while that at $\eta = 1$ would be equivalent to $\phi_{\theta_{xx}}$ when U_0 is replaced by $\bar{U}$.† With this proviso, the distributions of $(\omega L_u/U_0^2)\,\phi^*_{\theta_\beta}$ shown in figure 8 could, for $\eta = 1$, be identified with $\phi_{\theta_{xy}}$ and $\phi_{\theta_{xz}}$. These spectral densities rise more rapidly than $\phi_{\theta_{xx}}$ near the origin and reach a maximum at a frequency which is about 60 % of that at which

† $\bar{U} = \frac{1}{2}U_0$ at $\eta = 1$.

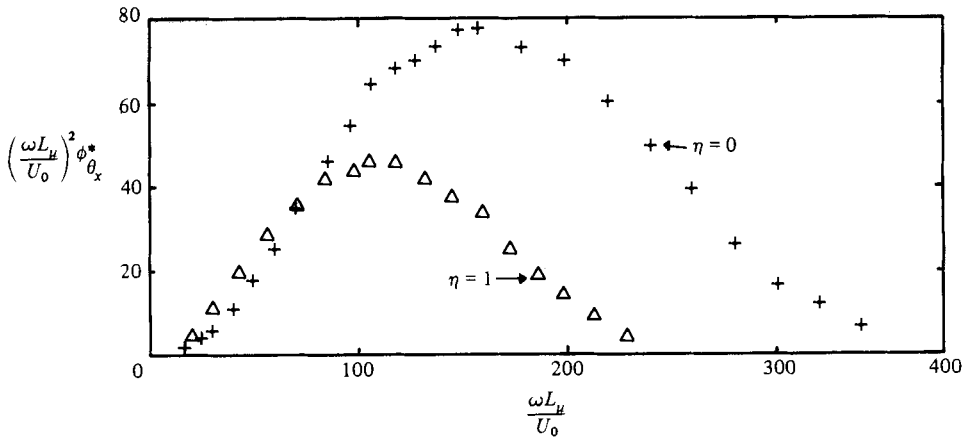

FIGURE 7. Spectral densities of the x-derivative of temperature weighted by the square of the frequency.

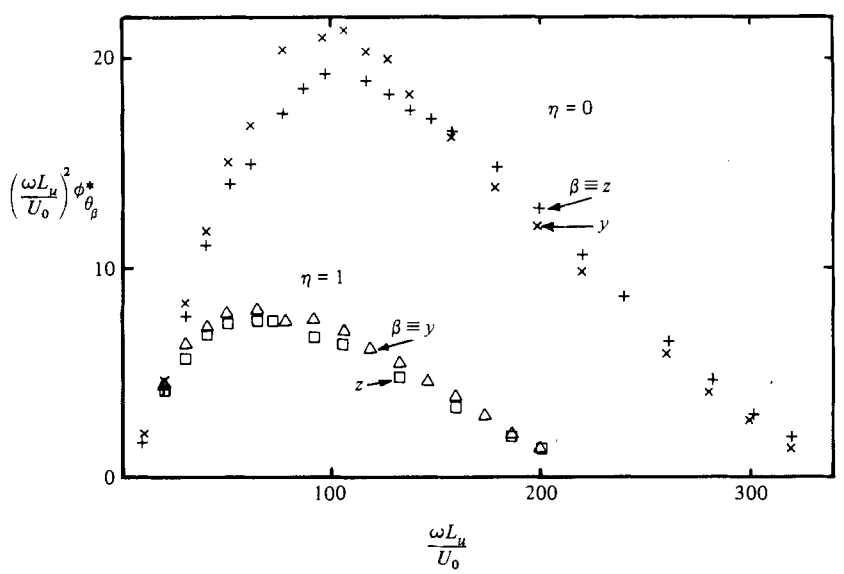

FIGURE 8. Spectral densities of the y- and z-derivatives of temperature weighted by the square of the frequency.

$\phi_{\theta xx}$ exhibits a peak. The difference (figures 7, 8) in the qualitative behaviour of $\phi_{\theta xy}$ (or $\phi_{\theta xz}$) and $\phi_{\theta xx}$ is however significantly smaller than that (figure 6) between ϕ_{θ_y} (or ϕ_{θ_z}) and ϕ_{θ_x}, reflecting the extra weighting given to the high-frequency end of the spectrum in the case of second-order derivatives. Spectra $\phi_{\theta xy}$ and $\phi_{\theta xz}$ are in reasonable agreement with each other, a result which is consistent with (13). The appropriately normalized mean-square values of $\partial^2\theta/\partial x\,\partial y$ and $\partial^2\theta/\partial x\,\partial z$, obtained by integrating the spectra of figure 8, are also in approximate agreement (figure 9†). While there is little variation in these quantities across the jet, $\overline{(\partial^2\theta/\partial x^2)^2}$ increases for $\eta > 0.5$. In the region $0 \leqslant \eta \lesssim 0.5$, the ratios $\overline{(\partial^2\theta/\partial x^2)^2}/\overline{(\partial^2\theta/\partial x\,\partial y)^2}$ and $\overline{(\partial^2\theta/\partial x^2)^2}/\overline{(\partial^2\theta/\partial x\,\partial z)^2}$ are equal to about 2.6, which is 13% smaller than the value

† A value of 2.05×10^{-5} m^2/s has been used for α.

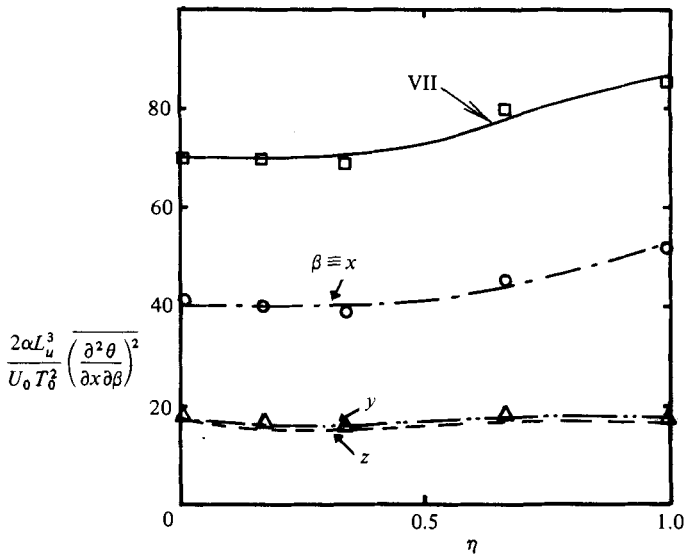

FIGURE 9. Term VII and its components. Symbols are individual data points; curves are least-square fits.

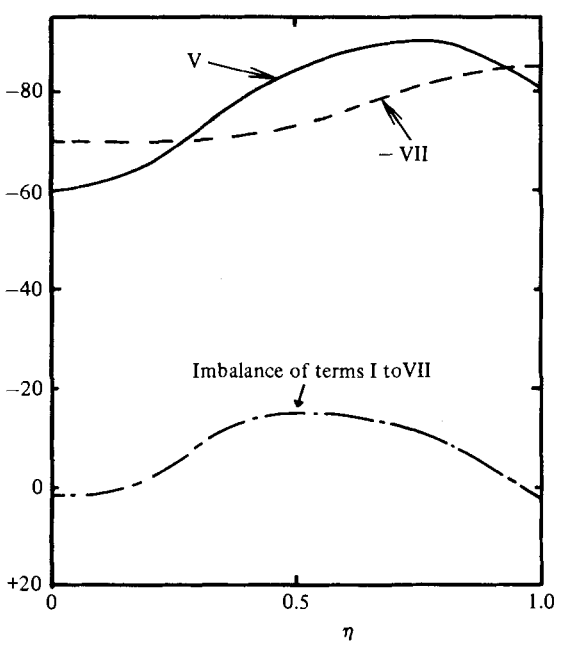

FIGURE 10. Terms V and VII and imbalance for the budget of $\overline{(\partial\theta/\partial x)^2}$. As for figure 4, the terms are normalized by $L_u^3/U_0 T_0^2$.

indicated by (9). Term VII, which is the sum of the three components of figure 9, exhibits a similar behaviour to $\overline{(\partial^2\theta/\partial x^2)^2}$ over the jet half-width. It is considerably larger than the terms in figure 4.

Term V, obtained with relation (6), is shown in figure 10. It is also considerably larger than the terms in figure 4 and exhibits a peak near $\eta = 0.8$; peaks in $\overline{uv}$, $\overline{v\theta}$ and production terms for $\overline{q^2}$ and $\overline{\theta^2}$ also occur near this location. The magnitude of

V is slightly smaller than that of VII, also shown in figure 10, near the jet centreline, but the trend is reversed for $\eta \gtrsim 0.3$. The imbalance, equal to the sum of terms I to VII, shown in figure 10, is satisfactorily small near $\eta = 0$ and $\eta = 1$ but increases to a maximum at $\eta \approx 0.5$. The magnitude of this maximum is larger than that of any of the terms in figure 4. An explanation for this imbalance could only be speculative until experimental verification of (6) becomes available. It should be noted, however, that the departure relative to local isotropy, between the three components of production, only needs to be of the same order as the measured departure for the components of dissipation. A departure from (6) would seem plausible in the light of the non-zero values of the correlations in figure 5. In particular, the non-zero values of the off-diagonal components of $\overline{(\partial\theta/\partial x_i)(\partial\theta/\partial x_j)}$ would seem consistent with an anisotropy in the term $\overline{(\partial\theta/\partial x_j)(\partial\theta/\partial x_k)(\partial u_k/\partial x_i)} + \overline{((\partial\theta/\partial x_i)(\partial\theta/\partial x_k)(\partial u_k/\partial x_j)}$, which may be interpreted as the source term in the transport equation for $\overline{(\partial\theta/\partial x_i)(\partial\theta/\partial x_j)}$.

It is important to note here that, although production and dissipation are large and of the same order, their difference tends to be of the same order as other terms in the $\overline{(\partial\theta/\partial x)^2}$ equation, and thus for predictive purposes all terms need to be considered. Unfortunately, the imbalance (figure 10) is perhaps too large *vis-à-vis* the terms in figure 4 to guide the construction of an accurate model for these latter terms.

There is a possibility that the departure from local isotropy, as reflected by the magnitude of $\overline{(\partial u/\partial x)(\partial\theta/\partial x)}$ and $\overline{(\partial\theta/\partial x)(\partial\theta/\partial y)}$, may be due to insufficiently large Reynolds and Péclet numbers for the present experiment. Spectra of second-order derivatives emphasize relatively high wavenumbers, and the components of the dissipation term exhibit only a relatively small (13 %) departure from local isotropy. Van Atta (1977) noted, on the basis of relatively small Reynolds-number boundary-layer measurements (Sreenivasan *et al.* 1977) of $\phi_{\theta x}$, $\phi_{\theta y}$ and $\phi_{\theta z}$, that for sufficiently high wavenumbers the temperature field is nearly locally isotropic with respect to second-order spectral quantities. In this latter flow, the ratio $\overline{(\partial\theta/\partial x)^2}/\overline{(\partial\theta/\partial\beta)^2}$ (with $\beta \equiv y$ or z) is significantly smaller than unity. In the present flow, the closer agreement with isotropy of $\overline{(\partial^2\theta/\partial x^2)^2}/\overline{(\partial^2\theta/\partial x\,\partial\beta)^2}$ than $\overline{(\partial\theta/\partial x)^2}/\overline{(\partial\theta/\partial\beta)^2}$ suggests moments of second derivatives are closer to isotropy than moments of first derivatives. This is not unreasonable, as the second derivative may be more effective at filtering the effects of anisotropy than the first derivative.

An indication of the location in the spectral domain of contributions by dissipation and production to the budget of $\overline{(\partial\theta/\partial x)^2}$ is given in figure 11. The contribution by all dissipation terms in VII is shown in that the dissipation spectrum $D(k_1 l_K)$, when integrated over all wavenumbers, is equal to $\overline{(\partial^2\theta/\partial x^2)^2} + \overline{(\partial^2\theta/\partial x\,\partial y)^2} + \overline{(\partial^2\theta/\partial x\,\partial z)^2}$. Only the spectral contribution from the first term of the production V is shown in figure 11, $Co(k_1 l_K)$ representing the cospectrum between $\partial u/\partial x$ and $(\partial\theta/\partial x)^2$ defined such that

$$\int_0^\infty Co(k_1 l_K)\,\mathrm{d}(k_1 l_K) = \overline{(\partial u/\partial x)(\partial\theta/\partial x)^2}.$$

Both D and Co have been multiplied by $k_1 l_K$ in figure 11 to give a meaningful indication of spectral contributions from term VII and the first term of V. The peaks in D and Co are less than one decade apart, and, while the contributions to D are confined to about one decade in the wavenumber range, contributions to Co are spread over more than two decades in wavenumber. This latter trend is similar to that reported by Mestayer (1982) (his figure 10*a*) for spectral contributions from the production and dissipation terms to $\overline{q^2}$ in a turbulent boundary layer. In his flow, R_λ was relatively high (≈ 600) and the peaks in production and dissipation were separated by about two decades. While there is little doubt that D has been shifted

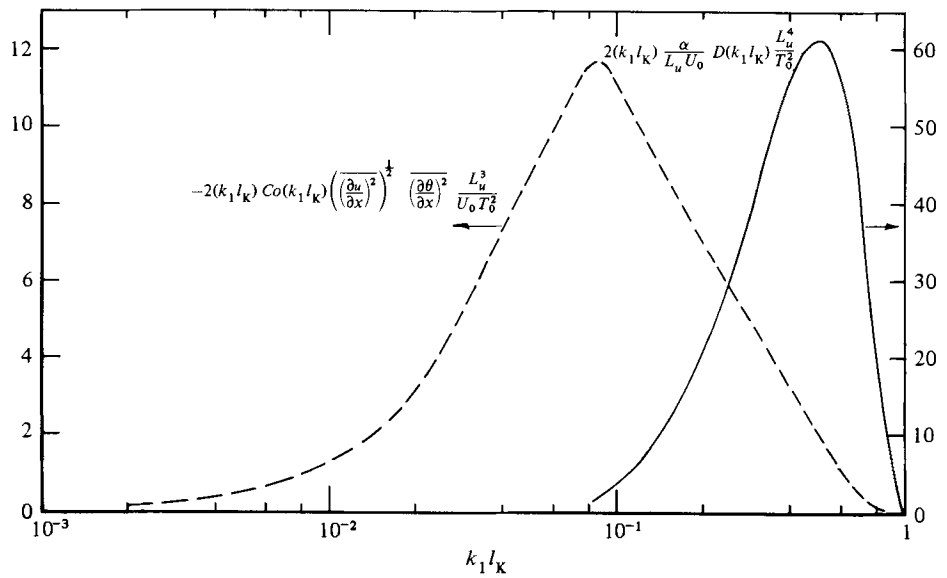

FIGURE 11. Spectral contributions to the budget of $\overline{(\partial\theta/\partial x)^2}$: ——, total dissipation (term VII); ——, first term of V (production) (note the different scales).

to higher frequencies, with respect to the dissipation of $\overline{q^2}$ (or presumably $\overline{\theta^2}$), this shift is evident also for the production, the peak in Co occurring at a wavenumber $k_1 l_K$ which is higher by a factor of almost 100 than that at which the production of $\overline{q^2}$ peaks (Mestayer 1982). The fact that the production of $\overline{(\partial\theta/\partial x)^2}$ no longer occurs in the strongly anisotropic part of the spectrum tends to corroborate the previous conclusion concerning the approach to isotropy of the dissipation terms of $\overline{(\partial\theta/\partial x)^2}$. A more detailed analysis of the small departures from local isotropy of the dissipation of $\overline{(\partial\theta/\partial x)^2}$ would be possible if a detailed spectral budget of $\overline{(\partial\theta/\partial x)^2}$ were available; such a budget has not been attempted here in view of the assumptions that would be required in connection with the production terms that have not been measured. It is worth noting, however, that all terms in the spectral budget of $\overline{\theta^2}$ are relatively easy to obtain experimentally; such a budget could help quantify the departures from local isotropy of the three dissipation components of $\overline{\theta^2}$.

The dominance of the transport equation for $\overline{(\partial\theta/\partial x)^2}$ by the production (due to fine-scale interactions) and dissipation terms mirrors the approximate balance between the production and dissipation terms in the isotropic form of the equation for the mean-square fluctuating vorticity (e.g. Champagne 1978). Champagne's results indicated the expected increase, with increasing Reynolds number, of both production and dissipation terms. The Reynolds-number behaviour of $\overline{(\partial u/\partial x)\,(\partial\theta/\partial x)^2}$, reported by Antonia & Chambers (1980), would suggest a Reynolds-number dependence of the important terms in the $\overline{(\partial\theta/\partial x)^2}$ budget analogous to that of the main terms in the vorticity fluctuation budget. It would be desirable to have measurements of the second derivatives for Reynolds numbers larger than in the present investigation to check whether or not the small departure from local isotropy persists. The present investigation does not provide an explanation for the relative magnitudes of the components of $\overline{N}$ and their possible variation with different flows. Consideration of the transport equations for $\overline{(\partial\theta/\partial y)^2}$ and $\overline{(\partial\theta/\partial z)^2}$, although difficult from a measurement viewpoint, should be a worthwhile subject for future investigation.

The assistance of Drs S. Rajagopalan, A. J. Chambers and D. Britz with the experiment and data reduction is gratefully acknowledged. The support of the Australian Research Grants Scheme is also gratefully acknowledged. The authors are also grateful to referees for their helpful comments.

REFERENCES

ANTONIA, R. A., BROWNE, L. W. B. & CHAMBERS, A. J. 1981 Determination of time constants of cold wires. *Rev. Sci. Instrum.* **52**, 107–110.

ANTONIA, R. A., BROWNE, L. W. B., CHAMBERS, A. J. & RAJAGOPALAN, S. 1983 Budget of the temperature variance in a turbulent plane jet. *Intl J. Heat Mass Transfer* **26**, 41–48.

ANTONIA, R. A. & CHAMBERS, A. J. 1980 On the correlation between turbulent velocity and temperature derivatives in the atmospheric surface layer. *Boundary-Layer Met.* **18**, 399–410.

ANTONIA, R. A., PHAN-THIEN, N. & CHAMBERS, A. J. 1980 Taylor's hypothesis and the probability density functions of temporal velocity and temperature derivatives in a turbulent flow. *J. Fluid Mech.* **100**, 193–208.

BATCHELOR, G. K. 1953 *The Theory of Homogeneous Turbulence.* Cambridge University Press.

BEGUIER, C., DEKEYSER, I. & LAUNDER, B. E. 1978 Ratio of scalar and velocity dissipation time scales in shear flow turbulence. *Phys. Fluids* **21**, 307–310.

BROWNE, L. W. B., ANTONIA, R. A. & RAJAGOPALAN, S. 1982 The spatial derivative of temperature in a turbulent flow and Taylor's hypothesis. *Phys. Fluids* **26**, 1222–1227.

CHAMPAGNE, F. H. 1978 The fine-scale structure of the turbulent velocity field. *J. Fluid Mech.* **86**, 67–108.

CORRSIN, S. 1953 Remarks on turbulent heat transfer: an account of some features of the phenomenon in fully turbulent regions. In *Proc. Thermodynamics Symposium, Iowa.*

ELGHOBASHI, S. & LAUNDER, B. E. 1981 Modeling the dissipation rate of temperature variance in a thermal mixing layer. In *Proc. 3rd Symp. on Turbulent Shear Flows, University of California at Davis*, pp. 15.13–15.17.

FREYMUTH, P. & UBEROI, M. S. 1971 Structure of temperature fluctuations in the turbulent wake behind a heated cylinder. *Phys. Fluids* **14**, 2574–2580.

LAUNDER, B. E. 1976 Heat and mass transport. In *Turbulence* (ed. P. Bradshaw), pp. 231–287. Springer.

LUMLEY, J. L. & KHAJEH-NOURI, B. 1974 Computational modeling of turbulent transport. *Adv. Geophys.* **18A**, 169–192.

MESTAYER, P. 1982 Local isotropy and anisotropy in a high-Reynolds-number turbulent boundary layer. *J. Fluid Mech.* **125**, 475–504.

MESTAYER, P. & CHAMBAUD, P. 1979 Some limitations to measurements of turbulence microstructure with hot and cold wires. *Boundary-Layer Met.* **16**, 311–329.

NEWMAN, G. R., LAUNDER, B. E. & LUMLEY, J. L. 1981 Modelling the behaviour of homogeneous scalar turbulence. *J. Fluid Mech.* **111**, 217–232.

OWEN, R. G. 1973 An analytical turbulent transport model applied to non-isothermal fully-developed duct flows. Ph.D. thesis, The Pennsylvania State University.

SREENIVASAN, K. R., ANTONIA, R. A. & DANH, H. Q. 1977 Temperature dissipation fluctuations in a turbulent boundary layer. *Phys. Fluids* **20**, 1238–1249.

SREENIVASAN, K. R. & TAVOULARIS, S. 1980 On the skewness of the temperature derivative in turbulent flows. *J. Fluid Mech.* **101**, 783–795.

TAVOULARIS, S. & CORRSIN, S. 1981 Experiments in nearly homogeneous turbulent shear flow with a uniform mean temperature gradient. Part 2. The fine structure. *J. Fluid Mech.* **104**, 349–367.

TENNEKES, H. & LUMLEY, J. L. 1972 *A First Course in Turbulence.* MIT Press.

VAN ATTA, C. W. 1974 Influence of fluctuations in dissipation rates on some statistical properties of turbulent scalar fields. *Izv. Atmos. Ocean. Phys.* **10**, 712–719.

VAN ATTA, C. W. 1977 Second-order spectral local isotropy in turbulent scalar fields. *J. Fluid Mech.* **80**, 609–615.

VEROLLET, E. 1972 Etude d'une couche limite turbulente avec aspiration et chauffage à la paroi. Thèse Doctorat ès Sciences, Université d'Aix-Marseille (also *Rapport* CEA-R-4872, 1977).

WYNGAARD, J. C. 1971 Effect of velocity sensitivity of temperature derivative statistics in isotropic turbulence. *J. Fluid Mech.* **48**, 763–769.

WYNGAARD, J. C. 1976 The maintenance of temperature derivative skewness in large Reynolds number turbulence. (Unpublished manuscript.)

WYNGAARD, J. C. & CLIFFORD, S. F. 1977 Taylor's hypothesis and high frequency turbulence spectra. *J. Atmos. Sci.* **34**, 922–929.